Atmospheric Pollution Research 5 (2014) 119-128

Atmospheric Pollution Research

www.atmospolres.com

Field evaluation of a near–real time elemental monitor and identification of element sources observed at an air monitoring supersite in Korea

Seung–Shik Park [1], Sung–Yong Cho [1], Mi–Ra Jo [2], Bu–Joo Gong [2], Jin–Soo Park [2], Suk–Jo Lee [2]

[1] *Department of Environment and Energy Engineering, Chonnam National University, 300 Yongbong–dong, Gwangju 500–757, Korea*
[2] *Air Quality Research Department, National Institute of Environmental Research, Kyungseo–dong, Seo–Gu, Incheon 404–170, Korea*

ABSTRACT

Ambient measurements of elemental species concentrations were made using an online elemental monitor at an air pollution monitoring station in Gwangju, Korea to evaluate the performance of the monitor for near–real time $PM_{2.5}$ elemental monitoring and identify possible sources of the observed elements. This study also demonstrates the utility of integrating hourly elemental data with the meteorological data to better understand the sources of elements. Good agreement between the online and filter–based measurements was obtained for the elements studied, with an R^2 of 0.73–0.97 and regression slopes of 0.84–2.37, suggesting the potential use of the online monitor to observe temporal variations in anthropogenic aerosol particles. Atmospheric element concentration levels studied were 2–20 times greater than their background levels when pollution plumes coming from industrial areas had impacted the site. Examination of the elements data revealed several short spikes of elements that are associated with local industrial emissions and road dusts. For the haze episodes observed over the study period, the element K was significantly influenced by biomass burning emissions with some impacts from soil dusts and industrial activities. Based on the wind direction and wind speed data, As/Se, Se/SO_4^{2-}, and correlations among Se, As, Pb, SO_2, and SO_4^{2-}, it is suggested that the observed As and Se were significantly impacted by local anthropogenic sources and long–range transport of aerosols, rather than local coal combustion or coke emissions. Conditional probability functions were applied to identify likely local emission source locations of the elements observed at the site, indicating that the elements contributions were from the southwest and northeast directions, where two industrial areas and an express highway are located. Results from principal component analysis indicate that the observed concentrations of the element species were likely attributed to road dust/local industrial emissions, oil combustion, and metal processing.

Keywords: *Near–real time elemental monitor, elements, As/Se and Se/SO_4^{2-} ratios, industrial emissions, principal component analysis*

doi: 10.5094/APR.2014.015

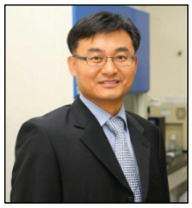

Corresponding Author:
Seung–Shik Park
☎ : *+82-62-530-1863*
🖷 : *+82-62-530-1859*
✉ : *park8162@chonnam.ac.kr*

Article History:
Received: 23 August 2013
Revised: 25 October 2013
Accepted: 08 November 2013

1. Introduction

It has been recognized that the exposure to elevated concentrations of particulate matter (PM) is associated with adverse human health effects (Dockery and Pope, 1994; Pope and Dockery, 2006). In particular, fine particles ($PM_{2.5}$) are more closely related to mortality and morbidity than coarse particles ($PM_{2.5–10}$) (Schwartz et al., 1996; Laden et al., 2000; Pope et al., 2002). Ambient PM is a complex mixture consisting of a number of chemical constituents such as carbonaceous, ionic, and elemental species.

Elemental species measurements of ambient aerosol particles, which are derived from anthropogenic (industrial facilities, incineration, vehicle exhaust, power plants, domestic heating, etc.) and natural (often crustal) sources, have been conducted for health and source apportionment studies. Elements including As, Sb, Cd, Cr, Hg, Pb and Be, have been identified as toxic air pollutants (Baird, 1995). It has also been suggested that some elements modulate the expression of pulmonary cytokines (Prieditis and Adamson, 2002; Schaumann et al., 2004) and are associated with oxidative stress in cell systems (Cheung et al., 2012). Elemental species are not significant contributors of $PM_{2.5}$ mass, but as the chemical composition of raw materials is reflected in the aerosol particles emitted, characteristic elements, which are called "marker species", have been employed to identify and apportion the source contributions to ambient aerosol (Kidwell and Ondov, 2004; Pancras et al., 2006; Snyder et al., 2009; Smyth et al., 2013). For example, Se is a unique tracer of primary particles from coal combustion (Morawska and Zhang, 2002), As is a tracer of metals–ore processing aerosol (Pancras et al., 2006; Park et al., 2006), Ni and V are tracers for oil combustion emissions (Ogulei et al., 2005), Fe and Mn are markers for steel mill emissions (Pancras et al., 2006), Sb is closely associated with brake wear emissions (Bukowiecki et al., 2009), and Cd, Zn and Cl are markers for municipal incinerator emissions (Ondov and Wexler, 1998; Suarez and Ondov, 2002).

Due to the reasons above, accurate measurements of the elemental composition of ambient aerosol particles are of much interest. Once the characteristic elements are associated with particular emission sources, real–time measurements can be made which provide detailed information about the emission characteristics of those sources. In addition, identification of short duration spikes in ambient concentrations of elemental species has been shown to indicate local sources of the emitted compounds (Pancras et al., 2006; Park et al., 2006; de Foy et al., 2012; Smyth et al., 2013). To provide improved temporal resolution of elemental species concentrations, sampling devices performing sub–hourly or hourly collection of ambient aerosol particles for subsequent

laboratory analysis have been developed and utilized in the field (Cahill and Wakabayashi, 1993; Kidwell and Ondov, 2001; Kidwell and Ondov, 2004; Lee et al., 2011; Park et al., 2012). These include the Davis Rotating–drum Unit for Monitoring (DRUM; Cahill et al., 1985), Semi–continuous Elements in Aerosol Sampler (SEAS; Kidwell and Ondov, 2001), and a Korean version of SEAS (KSEAS; Lee et al., 2011). All provide improved temporal resolution of elemental composition but require a large commitment of analytical time. To address the large analytical time commitment from semi–continuous sampling systems, online semi–continuous measurement systems such as Aerosol Time–of–Flight Mass Spectrometry (TSI ATOFMS, Shoreview, MN) and near–real time Xact 620 field XRF analyzer (Cooper Environmental Services, CES) have been developed and commercialized for rapid detection of the ambient aerosol particle's elemental composition. CES has reported the Xact 620 multi–elemental monitor with 1–hr sampling yielded equal to or better PM_{10} Pb measurements than 24–hr samples collected with PM_{10} FRM samplers and laboratory XRF analysis (www.cooperenvironmental.com). However the Xact elements monitor needs to be tested in more complex source environments to improve its performance.

Recently the Korean EPA has deployed intensive air pollution monitoring stations, which are similar to the U.S. EPA PM Supersites, to develop effective control strategies to reduce the impacts of atmospheric PM including Asian dusts and long–range transported aerosols. Details of Korean PM Supersites are described in Park et al. (2013). Currently the online field XRF monitors are being operated to observe temporal variations of elemental species at four air monitoring stations. A CES field XRF analyzer with hourly time–resolution was utilized to observe the temporal profiles of $PM_{2.5}$ elemental species during February of 2011 at a South Area Supersite in Gwangju, Korea. The objectives of this study are to (i) explore the accuracy of time–resolved CES multi–elements monitor by comparing with filter–based measurements, (ii) investigate the utility of integrating hourly elements data with meteorological data to provide a better understanding of the sources, and (iii) identify probable emission sources of the observed elemental species using a principle component analysis.

2. Methodology

2.1. Site description

The South Area Supersite (latitude 35.23°N, longitude 126.85°E) in Gwangju is located in the southern part of Korea, as depicted in Figure S1 of the Supporting Material (SM). A detailed description of the site can be found in Park et al. (2013). The site is located in a commercial and residential area which is surrounded by agricultural lands and traffic roads. The nearest major traffic road is approximately 0.3 km from the site, and an express highway is located 1.5–2.0 km southwest of the site. There is an industrial complex located 3–8 km southwest of the site (200–250°) and a high–tech industrial area located 1.0–1.5 km northeast (30–100°) of the site. It is important to note that there are no coal combustion boilers or industries that use coal within the industrial areas. The high–tech industrial area has a number of manufacturing companies, metallurgical companies, and chemical industries which account for 61.9%, 20.0%, and 3.4% of the total industries, respectively. Photonics and semi–conductor industries are also distributed within the complex. The industrial complex (southwest of the site) consists of approximately 1 000 industries of which 39.6 and 13.3% corresponded to metallurgical and chemical industries, respectively. Several large–scale companies producing household electric appliances are also distributed within the complex. There are also many small–scale companies producing car parts and metal coatings. Emissions from these industrial complex regions impacting the monitoring site could be resolved during typical southwestern and northeastern flow regimes. Meteorological data was monitored at the Gwangju regional meteorological station, located 7 km south of the site.

Time–resolved measurements of $PM_{2.5}$, organic and elemental carbon (OC and EC), ionic species, and elemental species were conducted at the Gwangju Supersite at 1–hr intervals during February 01–28, 2011. Only online XRF measurement results are discussed in this study. Water–soluble K^+ and SO_4^{2-} data are used as ancillary data to explore probable emissions sources of the elements studied.

2.2. 24–hr filter–based and hourly elemental species measurements

Twenty–four hour integrated filter–based $PM_{2.5}$ samples were collected between midnight and midnight with a sequential $PM_{2.5}$ sampler (PMS103, APM Korea) and then were analyzed by Energy Dispersive X–ray Fluouresence (EDXRF) spectrometer (Epsilon 5, PANalytical) for 29 elements (Si, S, K, Ca, Sc, Ti, V, Cr, Mn, Fe, Co, Ni, Cu, Zn, As, Se, Br, Rb, Sr, Mo, Cd, Sn, Sb, Te, Cs, Ba, Hg, Pb, and Bi). The Teflon filters (Teflon membrane, 2.0 μm pore size, R2PJ047, PALL Science, USA) were weighed before and after sample collections with a microbalance (1 μg sensitivity). In EDXRF, samples are energized by irradiation with X–rays, resulting in the emission of fluorescent X–rays with discrete energies characteristic of the elements present. The EDXRF spectrometer has an X–ray tube ($Power_{max}$=600 W, V_{max}=100 kV, Gd–anode), 3–dimensional polarization optics (Cartesian geometry), and Ge detector. The primary beam from the X–ray tube irradiates a polarizing target (secondary target) placed along the first axis of the optical path. After scattering at 90° the X–rays travel along the second axis to the filter sample. The spectrum of the sample is recorded by a detector placed along the third axis. By using secondary targets of different materials it is possible to optimize the excitation source for the elements of interest. In this study, we used eight secondary targets. The secondary targets, X–ray current and voltage were CaF_2: 17 mA and 35 kV; Ti: 8.5 mA and 70 kV; Fe: 7.5 mA and 80 kV; Ge: 7 mA and 85 kV; Zr: 6 mA and 100 kV; Mo: 6 mA and 100 kV; Ag: 6 mA and 100 kV; and Al_2O_3: 6 mA and 100 kV. X–ray counting time depends on the secondary target, ranging from 600 to 1 000 sec. The instrument was calibrated using thin film calibration standards (Micromatter – polycarbonate aerosol membranes, USA). The analytical target of analysis defines the necessary sample preparation technique. Diversity of sample type and measurement range is accommodated easily by the instrument. In this study filter samples were directly placed into the instrument. The quantifications of elements in the filter samples were carried out using an Auto Quantify routine based on fundamental parameters method. While a spectrum peak search and match routine facilities qualitative analysis. Spectrum evaluation was done by non–linear least squares fitting, based on the AXIL algorithm developed at the University of Antwerp, Belgium. The analysis time per filter sample was approximately 140 min. The filter blanks were also analyzed, and the average filter blank value was used as a background subtraction for each sample filter. Precision, defined as the relative standard deviation, was less than 10% for all elements. Minimum detection limit for each element analyzed by EDXRF was determined as three times the standard counting error of the background intensity, ranging from 0.25 to 5.98 ng/m^3.

Hourly $PM_{2.5}$ elemental concentrations of (K, Ca, Ti, V, Cr, Mn, Fe, Co, Ni, Cu, Zn, As, Se, Ag, Cd, Sn, Sb, Ba, Ag, Tl, and Pb) were measured with an ambient elemental monitor (model: Xact^{TM} 620, Cooper Environmental Services (CES), USA). The online Xact 620 monitor uses reel–to–reel filter tape sampling and nondestructive XRF analysis to measure ambient air particles. The air was introduced through a $PM_{2.5}$ inlet at a sampling flow rate of 16.7 L/min and drawn through the filter tape. The resulting $PM_{2.5}$ deposit was automatically advanced and analyzed by XRF for selected elemental species as the next sample was being collected. Sampling and analysis were performed continuously and simultaneously, except during advancement of the tape (~20 sec) and during daily automated quality assurance checks. The online Xact 620 monitor was calibrated using thin film standards for each

element of interest, which was provided by CES. These standards were manufactured by depositing vapor phase elements on blank Nuclepore (Micromatter Co., Arlington, WA, USA). The Nuclepore filter of known area was weighed before and after the vapor deposition process to determine the concentration (μg/cm^2) of each element. In this study, excellent agreement between the measured and standard masses for each element was observed, indicating a deviation of <±5%. The 1–hr time resolution minimum detection limits for K, Ca, Ti, V, Cr, Mn, Fe, Co, Ni, Cu, Zn, As, Se, Cd, Sn, Sb, Ba, Tl, and Pb were 0.81, 0.32, 0.18, 0.14, 0.11, 0.07, 0.08, 0.05, 0.04, 0.06, 0.04, 0.03, 0.03, 1.35, 2.54, 0.67, 0.40, 0.05, and 0.05 ng/m^3 respectively.

3. Results and Discussion

3.1. Comparison of hourly and 24–hr filter–based elemental measurements

The 24–hr averages of hourly elemental species measurements (K, Ca, Fe, Mn, Ti, Cu, V, Ni, Zn, As, Ba, and Pb) were compared with those derived from the laboratory XRF analysis of 24–hr integrated filter samples. Results are shown in Table 1 and Figure S2 (see the SM). Strong correlations were evident between elemental species concentrations measured by the two methods with R^2 ranging from 0.73 (Ti) to 0.97 (K and Zn), with the exception of V (R^2=0.46). However, regression slopes between the measured concentrations from both methods varied greatly (0.84 (Ti) to 2.37 (Ca)). Cu, Zn and Pb which are typically emitted from anthropogenic sources had good linear relationships between the methods with slopes of 1.18 (R^2=0.96), 1.14 (R^2=0.97), and 1.11 (R^2=0.94), respectively. K, which has been used as a marker of soil dusts and biomass burning (K^+) emissions, showed excellent linearity with a slope of 1.06. Online XRF measurement results for the elements Ca (2.37) and Fe (1.56) were significantly overestimated compared to the filter–based measurements, but the field deployed XRF analyzer may be a viable candidate for time–resolved quantification of PM concentration spikes of elemental species from a variety of industrial facilities. In this study, the good agreement between the trace element constituents reported by the two methods was found during the limited period of measurement, but long–term measurements of elements, i.e. over a year period, are needed to evaluate the performance of the online elements monitor with varying meteorological and air pollution conditions.

3.2. Temporal profiles of hourly element species and their sources

Figure S3 (see the SM) shows temporal profiles of K^+, K^+/K, As, and Se concentrations over the study period. Hourly K and K^+ concentrations were 877±989 ng/m^3 (40–5 892) and 820±985 ng/m^3 (67–5 570), respectively. Maximum concentrations of K (5 892) and K^+ (5 570) were approximately 15 and 19 times higher than their background concentrations (420 and 300 ng/m^3) which were observed prior to the onset of an excursion. The K^+/K ratio was relatively high, ranging from 0.22 to 1.09, and showed typically temporal variation similar to K^+. For the concentration of K^+ exceeding 2 000 ng/m^3, the K^+/K ratio was above 0.8. High K^+/K ratio indicates the significant contribution from biomass burning (Shen et al., 2007; Park et al., 2013). A strong relationship between total K and K^+ (*slope*=0.81; R^2=0.96, not shown here) also suggest that the observed concentrations of these two chemical species were clearly attributed to similar sources. As and Se concentrations were 11.7±7.3 ng/m^3 (0.1–34.0) and 4.3±3.1 ng/m^3 (0.4–13.5) ng/m^3, respectively. Their maximum levels were approximately 6 and 4 times higher than the respective background levels (5.9 and 3.2 ng/m^3). Hourly ambient concentrations of As and Se over the study period were highly correlated with a slope of 3.04±1.63 (0.16–13.82) and an R^2 of 0.65 (not shown here), suggesting that these two elements were from similar sources. Also a strong correlation of Se with Pb (R^2=0.77) was observed (not shown here). Possible sources of the As and Se observed at the site are discussed in detail below.

Figures 1 and 2 show time–series measurements of meteorology (wind direction and speed) and semi–continuous element concentrations (K, Ca, Fe, Zn, As, Cd, Se, Sb, Ba, and Pb) during two haze periods of February 01 to 08 (the first haze episode) and February 16 to 21 (the second haze episode), which occurred over the study period. Detailed description for the first episode is given elsewhere (Park et al., 2013). Local winds during the first episode came from southwest direction (210–280°) with wind speeds of 0.1–3.7 m/s (an average of 1.1 m/s). During the second haze episode, winds came predominantly from southwest or southeast direction with wind speeds ranging from 1.0 to 3.0 m/s. As shown in Figures 1 and 2, emission plume events from the southwest and northeast industrial areas were evident at the monitoring site. Elemental concentrations observed during these two episodes were high relative to background levels. For example, As and Se concentrations during the first episode when winds came continuously from the direction of 210–270°, which brought air from the industrial complex where many metallurgical and chemical industries are located, remained high (Figure 1). Also during the nighttime hours on February 18th (second episode) when the wind direction was from the industrial area, Fe, Zn, Cd, Sb, Ba, and Pb concentrations were high compared to their background concentrations (see Figure 2). Another event occurred during the night on February 20th when the local winds were from the southwest and resulted in increased K, Ca, Fe, Zn, Sb, Ba, and Pb concentrations. However, the elements data obtained from the limited measurement periods do not allow an assessment of the monthly and seasonal variability of the sources and composition of elemental species at this site that is impacted from local industrial emission sources and transport from China. Accordingly, in the future, more studies are required to better understand the seasonal and monthly variability of elemental sources at the site.

Table 1. *Comparison of 24–hr average online and filter–based elemental measurements*

Elements	Filter–based (ng/m^3) (x)	Online–based (ng/m^3) (y)	Regression relationship	R^2
K	715±727	732±780	y=(1.06±0.04)^a x + (-21.20±43.03)	0.97
Ca	70±28	122±74	y=(2.37±0.24)^a x + (-43.46±17.81)	0.83
Fe	198±73	293±122	y=(1.56±0.13)^a x + (-16.21±27.98)	0.87
Mn	20±9	24±12	y=(1.25±0.08)^a x + (-0.42±1.66)	0.93
Ti	10.0±5.2	8.7±4.4	y=(0.84±0.09)^a x + (0.74±1.09)	0.73
Cu	9.8±6.1	15.5±7.4	y=(1.18±0.06)^a x + (3.96±0.65)	0.96
V	3.3±2.2	4.6±1.6	y=(0.48±0.14)^a x + (3.05±0.53)	0.46
Ni	2.4±1.1	3.8±1.5	y=(1.24±0.14)^a x + (0.78±0.36)	0.81
Zn	94±50	103±57	y=(1.14±0.05)^a x + (-4.30±5.13)	0.97
As	7.1±3.1	9.6±5.1	y=(1.51±0.14)^a x + (-1.11±1.10)	0.85
Ba	27±39	52±46	y=(1.15±0.07)^a x + (21.09±3.46)	0.95
Pb	41±31	49±36	y=(1.11±0.06)^a x + (2.97±3.07)	0.94

^{a} *indicate p<0.01*

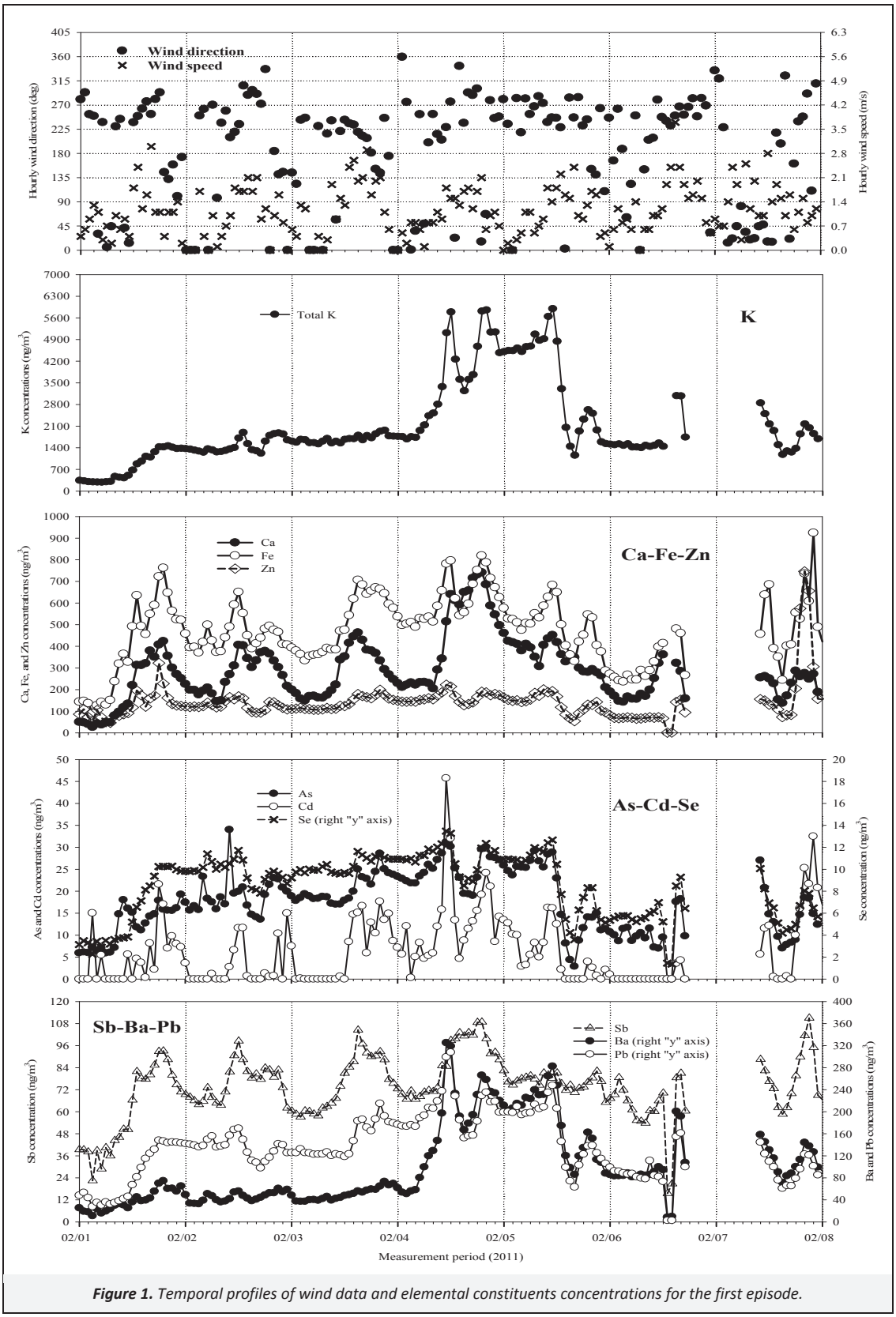

Figure 1. *Temporal profiles of wind data and elemental constituents concentrations for the first episode.*

To assess probable emissions sources of the observed K, As, and Se during the two pollution episodes, relationships of K with K^+, Ca, Fe, and Mn were examined, results of which are shown in Figure 3. Also relationships of Se with As and SO_2 are included in Figure 3. During the first episode, a strong correlation between K and K^+ (a slope of 0.82 and an R^2 of 0.96) and moderate correlations of K with Ca (R^2=0.56), Fe (R^2=0.36), and Mn (R^2=0.41), which are indicative of soil dust emissions, were observed. The K during the second episode was correlated with K^+ (a slope of 0.70), Ca, Fe, and Mn, with R^2 of 0.68, 0.44, 0.46 and 0.30, respectively. Consequently, results from the regression analyses suggest that the observed K during the two episodes were contributed from biomass burning emissions with some influence from soil dusts, with higher contribution of K^+ from biomass burning emissions during the first episode than during the second episode.

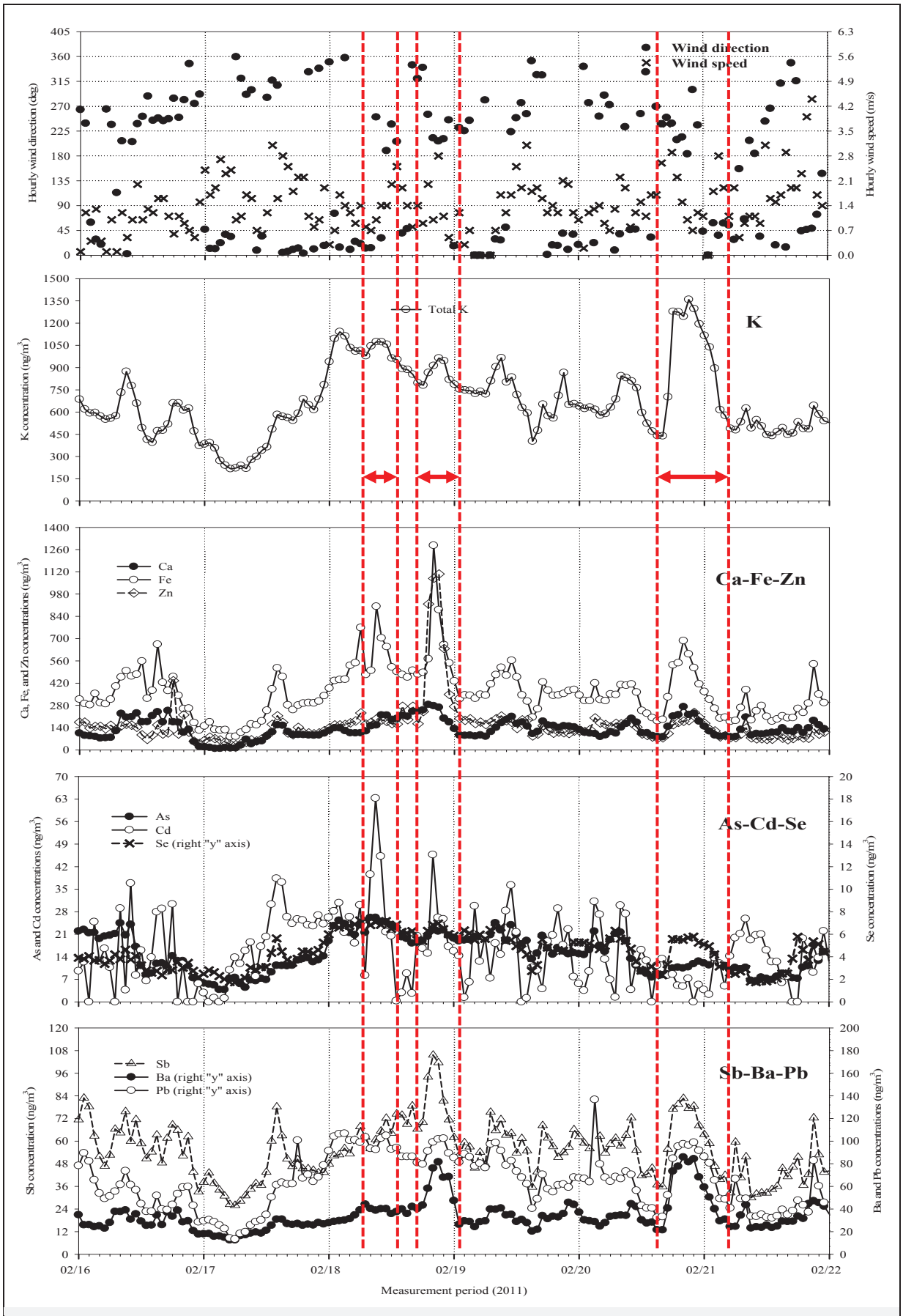

Figure 2. *Temporal profiles of wind data and elemental constituents concentrations for the second episode.*

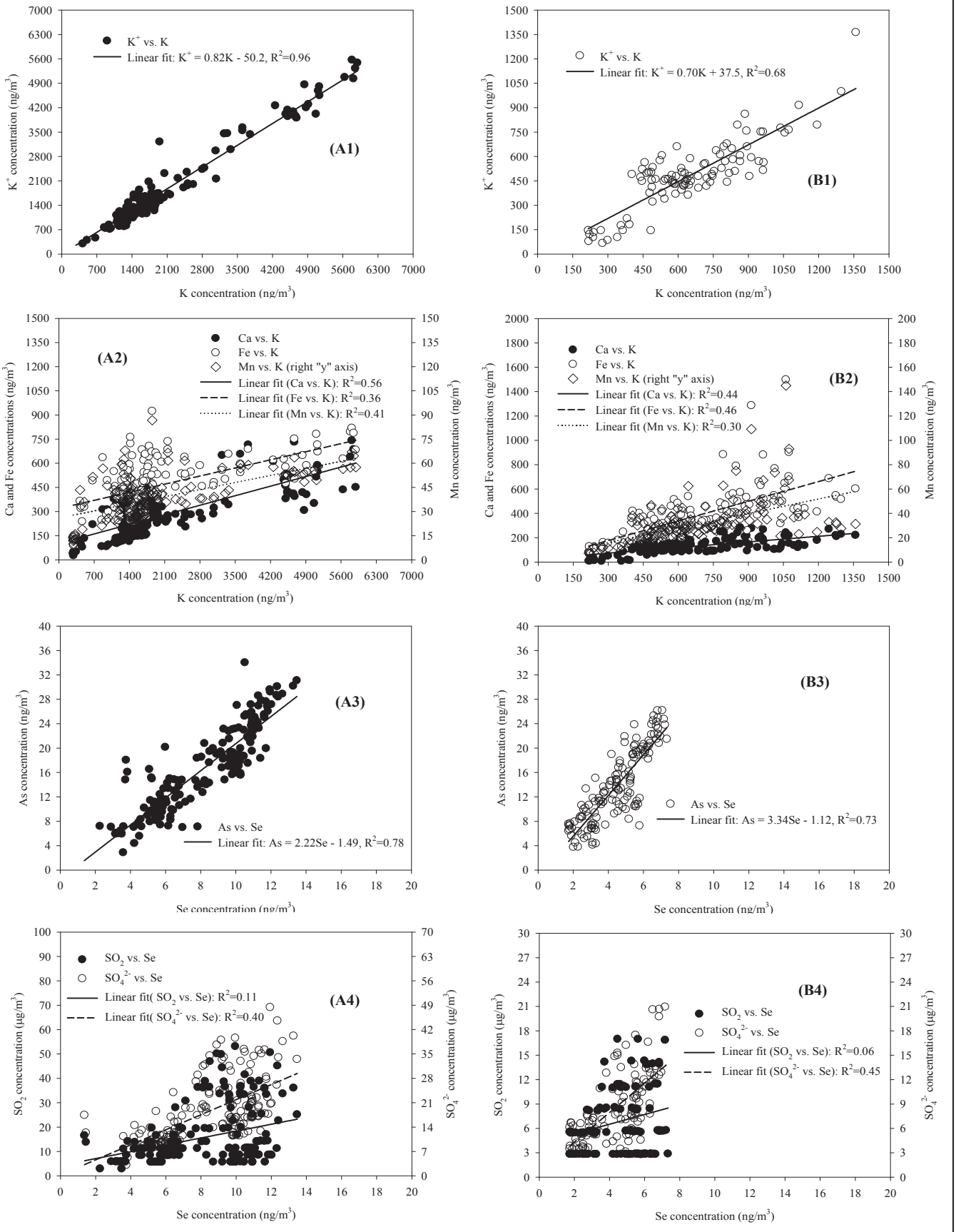

Figure 3. *Regression analyses among K, K^+, Ca, Fe, Mn, As, Se, SO_2, and SO_4^{2-}; (A1)–(A4) and (B1)–(B4) indicate the first and second episodes, respectively.*

It has been reported that Se and SO_2 are good indicators of coal combustion or coke emissions (Morawska and Zhang, 2002; Ogulei et al., 2005; Park et al., 2006), with a high Se/SO_4^{2-} ratio in a freshly emitted plume. Moreover, the As/Se ratio of ~1.0 is reported in air sheds influenced by coal combustion and has been used to distinguish between the influences of coal combustion and other anthropogenic sources (Park et al., 2006). In this study, As/Se and Se/SO_4^{2-} ratios were 2.0±0.5 (0.8–4.8) and 0.001±0.0002 (0.000–0.001) for the first episode, and 3.2±0.7 (1.3–4.9) and 0.001±0.0002 (0.000–0.002) for the second episode, respectively. Low Se/SO_4^{2-} ratios (<0.001) observed in the present study suggest plumes that have undergone sufficient atmospheric dilution or other anthropogenic emission sources of Se rather than coal combustion. The Se was strongly correlated with As and Pb with R^2 of 0.78 (a slope of 2.2) and 0.85 (not shown here) for the first episode, and of 0.73 (a slope of 3.3) and 0.79 (not shown here) for the second episode, respectively, implying their influence from similar sources. The observed Se was also correlated with SO_2 and SO_4^{2-} with R^2 of 0.11 and 0.40 for the first episode, and with R^2 of 0.06 and 0.45 for the second episode, respectively, suggesting that both Se and SO_2 were not derived from similar emission sources. However, considering the significant contribution of SO_4^{2-} from long–range transport of air pollutants at the site during winter (Cho and Park, 2013; Park et al., 2013), moderate correlations between Se and SO_4^{2-} suggest some influence of Se from long–range transported aerosols. Therefore, during the two episodes, high As/Se (>2.0), low Se/SO_4^{2-}, and correlations among Se, As, Pb, SO_2, and SO_4^{2-} suggest significant contributions of the As and Se from other anthropogenic local sources rather than coal combustion, with some contribution of corresponding elemental species from long–range transport of aerosols.

3.3. Enrichment factor and conditional probability function analyses

Enrichment factor (EF) analyses of elemental species were performed to assess the origin of the elements, i.e., natural or anthropogenic origin (see S1 of the SM). Figure S4 shows enrichment factor of the element species. As shown in Figure S4 (see the SM), the EF values for Ti and Fe were less than 2, suggesting that these elements were dominated by crustal origin. Also concentrations of K (r=0.84), Ti (r=0.90), Mn (r=0.90), Fe (r=0.71), and Ba (r=0.79) were strongly related to Ca, the reference crustal element, indicating that these elements were likely associated with crustal sources. Elements K, Mn, and Ba, which are derived from soil dust emissions, had EF values of 10–30, suggesting also some contributions from anthropogenic emissions to these elements. For example, Mn is from metal processing (Pancras et al., 2006; Heo et al., 2009) and Ba from brake wear (Bukowiecki et al., 2009). Compared with the dust–derived elements, large EF values were found for pollution elements, i.e., Cu, Zn, As, Se, Cd, Sb, and Pb, reflecting the influence of anthropogenic emissions.

A conditional probability function (CPF) was utilized to identify likely locations of local emission sources affecting concentrations of element constituents at the sampling site (see S2 of the SM). Figure 4 shows the CPF concentration plots of K, Fe, Cu, Zn, As, Se, Cd, Sb, and Pb when the 75^{th} percentile of their concentrations was set as the threshold criterion. The emission sources are likely located in the directions that have high conditional probability values. Park et al. (2013) indicated that in addition to industrial sources, the observed concentrations of Sb, Fe, Ca, Cr, Mn, Zn, Ba, and Pb were attributed to road dust associated with traffic abrasion processes such as engine wear, brake wear, and tire wear. Studies have also shown that Ca, Ti, Zn, Sn, Sb, Ba, and Pb are primarily derived from vehicular wear processes such as brake (Sb, Ba, Zn, Cu) and tire wear (Zn) and motor oil additives (Ca) (Lough et al., 2005; Bukowiecki et al., 2009). Elements associated with both steel and vehicular sources include Fe, Ba, Cu, and Zn (Sternbeck et al., 2002; Sanders et al., 2003). CPF results for K, Fe, Cu, Zn, Sb, and Pb suggest that source association could likely be from southwest or westerly (200–290°) emissions, where an express highway is situated, and these observations were partially attributable to motor vehicle wear processes. CPF directionalities suggest that some of the observed concentrations of these elements may have been transported from the industrial complexes to the site. High CPF values of Fe, Mn (not shown here), Cu, Zn, and Pb suggest contributions from metal processing, unique of industrial emissions (Heo et al., 2009). Source directions are pointing to the southwest where various industries including motor and metal processing facilities and electronics are located. In addition to the southwest direction, CPF plots point northeast where a high–tech industrial area is located. In summary, part of the observed concentration of K, Fe, Mn, Cu, Zn, As, Se, Cd, and Pb were likely apportioned to industrial sources which can be attributed to local manufacturing emissions from northeast and southwest wind directions.

3.4. Identification of elemental emission sources using a principal component analysis

A principle component analysis (PCA) with VARIMAX rotation (SPSS, v20.0) was performed to identify possible emission sources of the element constituents observed during the one month sampling period. Carbon monoxide (CO), elemental carbon (EC), organic carbon (OC), K, Ca, Fe, Ti, V, Cr, Mn, Ni, Cu, Zn, As, Se, Cd, Sb, Ba, and Pb were used for the PCA analysis. In this analysis, inclusion of carbonaceous species was to examine the relationship of traffic source with road dust emissions. Three principle components with eigenvalue greater than 1.0 were extracted, and explained 81.3% of the total variance in the data set (Table 2). PC1 accounts for 43.5% of the total variance and had high component loadings for CO, K, Ca, Ti, Cr, Cu, As, Se, Sb, Ba, and Pb, along with moderate loadings for EC, OC, Fe, and Zn, likely representing road dust (crustal elements + brake and tire wear processes) associated with traffic emissions (CO, EC, and OC). High and moderate loadings for As, Se, Pb, Cr, K, Fe, Mn, Cu, and Zn which appeared in the PC1 may be a result of industrial emission sources (refuse and municipal incineration, metal–related industries, etc.) from the southwest where an industrial complex is located. PC2 explained 19.5% of the total variance, and is highly loaded with the fuel oil markers V and Ni, along with moderate loadings of CO, EC, and OC components, which are likely associated with combustion sources. PC3 is associated with high component loadings for Fe, Mn, Zn, and Cd, along with moderate loadings for Cu and Pb. This indicates contributions from metal processing (Heo et al., 2009). There are many small–scale companies involved with car parts production, metal plating and steel processing in the southwest of the site. There are also manufacturing, metallurgical and chemical industries located northeast of the monitoring site. In conclusion, the PCA results clearly demonstrate the directionality of the observed element species using CPF.

4. Conclusions

Near–real–time measurements of element species in $PM_{2.5}$ were made using a CES (Cooper Environmental Services) field XRF analyzer for one month at a South Area Supersite in Gwangju, Korea. Accuracy of the XRF measurements was compared to filter–based method and the data were used to identify probable emission sources of the observed element concentrations. Element species concentrations from the field XRF monitor were strongly correlated with the filter–based method results, with R^2 ranging from 0.73 (Ti) to 0.97 (K) and regression slopes from 0.84 (Ti) to 2.37 (Ca). Results demonstrate the online field XRF analyzer may be utilized to detect concentration spikes of element species in anthropogenic plumes from a variety of industrial processes.

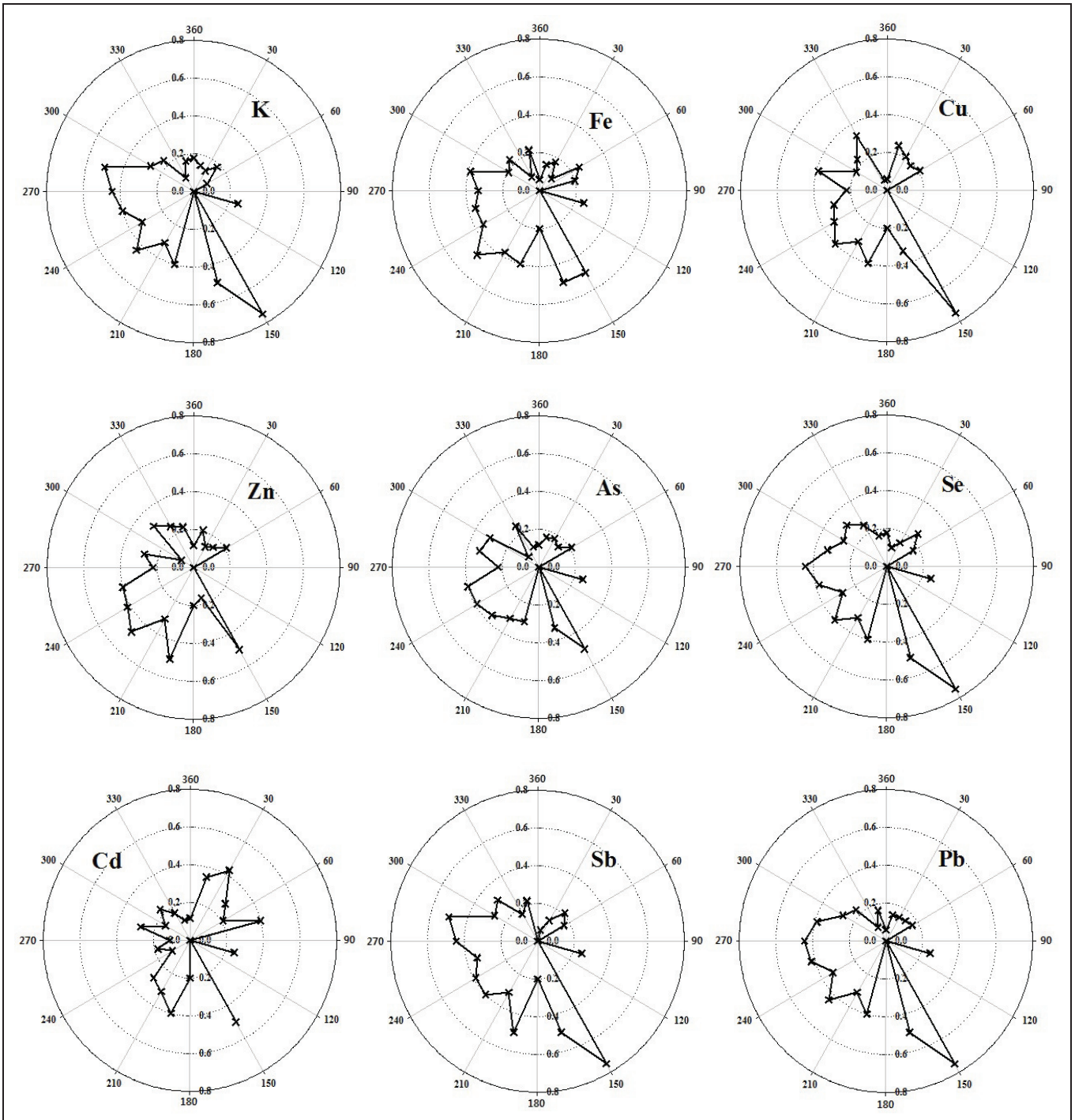

Figure 4. *CPF plots for the 75th percentile of K, Fe, Cu, Zn, As, Se, Cd, Sb and Pb concentrations.*

Time–resolved measurements revealed that intermittent short time frame element spikes were associated with industrial complex emissions. It is suggested that the abundances of As and Se observed at the site were likely attributed to more local anthropogenic industrial sources and long–range transport of aerosols than coal combustion or coke emissions, which were evidenced by the wind data, As/Se, Se/SO_4^{2-}, and correlations among Se, As, Pb, SO_2, and SO_4^{2-}. A conditional probability function (CPF) was used to identify likely local emission source locations of the elements observed at the site. The CPF indicated that elements contributions to the site were mostly coming from the southwest and northeast directions, where two industrial areas and an express highway are located. According to the K^+/K, enrichment factor analysis and CPF, the observed K could be influenced by significant contribution from biomass burning emissions, along with some influence from soil dusts and industrial source emissions. Principal component analysis (PCA) was applied to the data matrix of 620 samples and 19 variables to extract probable emission sources of the observed elements. Three principle components were extracted; road dust (crustal elements + traffic abrasion processes)/local industrial emissions, oil combustion, and metal processing.

Table 2. *Results of principal component analysis after VARIMAX rotation*

	PC1	PC2	PC3	Communality
CO	**0.706**	0.571	0.105	0.836
EC	0.579	0.520	0.335	0.718
OC	0.590	0.526	0.379	0.768
K	**0.929**	0.186	0.045	0.900
Ca	**0.897**	0.121	0.215	0.865
Fe	0.552	0.351	**0.694**	0.909
Ti	**0.787**	0.229	0.321	0.775
V	0.137	**0.867**	0.015	0.771
Cr	**0.769**	0.407	0.396	0.914
Mn	0.482	0.304	**0.694**	0.807
Ni	0.347	**0.837**	0.256	0.885
Cu	**0.613**	0.257	0.504	0.696
Zn	0.535	0.393	**0.646**	0.857
As	**0.654**	0.404	0.287	0.674
Se	**0.783**	0.541	0.065	0.910
Cd	-0.127	-0.175	**0.827**	0.730
Sb	**0.672**	0.397	0.385	0.758
Ba	**0.881**	0.130	0.102	0.804
Pb	**0.762**	0.092	0.521	0.861
Eigenvalue	8.27	3.70	3.48	15.44
Variance (%)	43.5	19.5	18.3	
Probable source type	Road dust/ industrial sources	Oil combustion	Metal processing	

Loadings > 0.6 (high) are in bold and loadings > 0.5 (moderate) are underlined.

Acknowledgments

This work was supported by project "Investigation on chemical characteristics of $PM_{2.5}$ and its formation processes by areas" funded from the National Institute of Environmental Research. This work was also partially supported by the General Researcher Program through a NRF grant funded by the Korea government (MEST) (NRF–2011–0007222).

Supporting Material Available

Enrichment factor analysis (S1), Conditional probability function (S2), Area map of Gwangju PM Supersite (Figure S1), Comparison between online and filter–based elemental measurements (Figure S2), Temporal profiles of K^+, K^+/K, As, and Se over the entire study period (Figure S3), Enrichment factor of elemental species in $PM_{2.5}$ (Figure S4), and General patterns of wind directions during the study period (Figure S5). This information is available free of charge via the Internet at http://www.atmospolres.com.

References

Baird, C., 1995. *Environmental Chemistry*, 2nd Edition, W.H. Freeman and Company, New York, pp. 347–381.

Bukowiecki, N., Lienemann, P., Hill, M., Figi, R., Richard, A., Furger, M., Rickers, K., Falkenberg, G., Zhao, Y.J., Cliff, S.S., Prevot, A.S.H., Baltensperger, U., Buchmann, B., Gehrig, R., 2009. Real–world emission factors for antimony and other brake wear related trace elements: Size–segregated values for light and heavy duty vehicles. *Environmental Science & Technology* 43, 8072–8078.

Cahill, T.A., Wakabayashi, P., 1993. Compositional analysis of size–segregated aerosol samples, *in Measurement Challenges in Atmospheric Chemistry*, edited by Newman, L., Advanced Chemistry Series No. 232, American Chemical Society, Washington, DC, pp. 211–228.

Cahill, T.A., Goodart, C., Nelson, J.W., Eldred, R.A., Nasstrom, J.S., Feeny, P.J., 1985. Design and evaluation of the DRUM impactor. Editors Ariman, T., Veziroglu, T.N., *Proceedings of the International Symposium on Particulate and Multi–Phase Processes,* Vol. 2 Taylor and Francis, Philadelphia, pp. 319–325.

Cheung, K., Shafer, M.M., Schauer, J.J., Sioutas, C., 2012. Diurnal trends in oxidative potential of coarse particulate matter in the Los Angeles Basin and their relation to sources and chemical composition. *Environmental Science & Technology* 46, 3779–3787.

Cho, S.Y., Park, S.S., 2013. Resolving sources of water–soluble organic carbon in fine particulate matter measured at an urban site during winter. *Environmental Science–Processes & Impacts* 15, 524–534.

de Foy, B., Smyth, A.M., Thompson, S.L., Gross, D.S., Olson, M.R., Sager, N., Schauer, J.J., 2012. Sources of nickel, vanadium and black carbon in aerosols in Milwaukee. *Atmospheric Environment* 59, 294–301.

Dockery, D.W., Pope, C.A., 1994. Acute respiratory effects of particulate air–pollution. *Annual Review of Public Health* 15, 107–132.

Heo, J.B., Hopke, P.K., Yi, S.M., 2009. Source apportionment of $PM_{2.5}$ in Seoul, Korea. *Atmospheric Chemistry and Physics* 9, 4957–4971.

Kidwell, C.B., Ondov, J.M., 2004. Elemental analysis of sub–hourly ambient aerosol collections. *Aerosol Science and Technology* 38, 205–218.

Kidwell, C.B., Ondov, J.M., 2001. Development and evaluation of a prototype system for collecting sub–hourly ambient aerosol for chemical analysis. *Aerosol Science and Technology* 35, 596–601.

Laden, F., Neas, L.M., Dockery, D.W., Schwartz, J., 2000. Association of fine particulate matter from different sources with daily mortality in six U.S. cities. *Environmental Health Perspectives* 108, 941–947.

Lee, D.S., Lee, B., Eom, J.W., 2011. A compact semi–continuous atmospheric aerosol sampler for elemental analysis: A preliminary result. *Atmospheric Pollution Research* 2, 506–512.

Lough, G.C., Schauer, J.J., Park, J.S., Shafer, M.M., Deminter, J.T., Weinstein, J.P., 2005. Emissions of metals associated with motor vehicle roadways. *Environmental Science & Technology* 39, 826–836.

Morawska, L., Zhang, J.F., 2002. Combustion sources of particles. 1. Health relevance and source signatures. *Chemosphere* 49, 1045–1058.

Ogulei, D., Hopke, P.K., Zhou, L.M., Paatero, P., Park, S.S., Ondov, J., 2005. Receptor modeling for multiple time resolved species: The Baltimore, supersite. *Atmospheric Environment* 39, 3751–3762.

Ondov, J.M., Wexler, A.S., 1998. Where do particulate toxins reside? An improved paradigm for the structure and dynamics of the urban mid–Atlantic aerosol. *Environmental Science & Technology* 32, 2547–2555.

Pancras, J.P., Ondov, J.M., Poor, N., Landis, M.S., Stevens, R.K., 2006. Identification of sources and estimation of emission profiles from highly time–resolved pollutant measurements in Tampa, FL. *Atmospheric Environment* 40, S467–S481.

Park, S.S., Jung, S.A., Gong, B.J., Cho, S.Y., Lee, S.J., 2013. Characteristics of $PM_{2.5}$ haze episodes revealed by highly time–resolved measurements at an air pollution monitoring supersite in Korea. *Aerosol and Air Quality Research* 13, 957–976.

Park, S.S., Ko, J.M., Lee, D.S., 2012. Application of semi–continuous ambient aerosol collection system for elemental analysis. *Journal of Korean Society for Atmospheric Environment* 28, 39–51 (in Korean).

Park, S.S., Pancras, J.P., Ondov, J.M., Robinson, A., 2006. Application of the pseudo–deterministic receptor model to resolve power plant influences on air quality in Pittsburgh. *Aerosol Science and Technology* 40, 883–897.

Pope, C.A., Burnett, R.T., Thun, M.J., Calle, E.E., Krewski, D., Ito, K., Thurston, G.D., 2002. Lung cancer, cardiopulmonary mortality, and long–term exposure to fine particulate air pollution. *JAMA–Journal of the American Medical Association* 287, 1132–1141.

Pope, C.A., Dockery, D.W., 2006. Health effects of fine particulate air pollution: Lines that connect. *Journal of the Air & Waste Management Association* 56, 709–742.

Prieditis, H., Adamson, I.Y.R., 2002. Comparative pulmonary toxicity of various soluble metals found in urban particulate dusts. *Experimental Lung Research* 28, 563–576.

Sanders, P.G., Xu, N., Dalka, T.M., Maricq, M.M., 2003. Airborne brake wear debris: Size distributions, composition, and a comparison of dynamometer and vehicle tests. *Environmental Science & Technology* 37, 4060–4069.

Schaumann, F., Borm, P.J.A., Herbrich, A., Knoch, J., Pitz, M., Schins, R.P.F., Luettig, B., Hohlfeld, J.M., Heinrich, J., Krug, N., 2004. Metal–rich ambient particles (particulate matter 2.5) cause airway inflammation in healthy subjects. *American Journal of Respiratory and Critical Care Medicine* 170, 898–903.

Schwartz, J., Dockery, D.W., Neas, L.M., 1996. Is daily mortality associated specifically with fine particles? *Journal of the Air & Waste Management Association* 46, 927–939.

Shen, Z.X., Cao, J.J., Arimoto, R., Zhang, R.J., Jie, D.M., Liu, S.L., Zhu, C.S., 2007. Chemical composition and source characterization of spring aerosol over Horqin sand land in northeastern China. *Journal of Geophysical Research* 112, D14315.

Smyth, A.M., Thompson, S.L., de Foy, B., Olson, M.R., Sager, N., McGinnis, J., Schauer, J.J., Gross, D.S., 2013. Sources of metals and bromine–containing particles in Milwaukee. *Atmospheric Environment* 73, 124–130.

Snyder, D.C., Schauer, J.J., Gross, D.S., Turner, J.R., 2009. Estimating the contribution of point sources to atmospheric metals using single–particle mass spectrometry. *Atmospheric Environment* 43, 4033–4042.

Sternbeck, J., Sjodin, A., Andreasson, K., 2002. Metal emissions from road traffic and the influence of resuspension—results from two tunnel studies. *Atmospheric Environment* 36, 4735–4744.

Suarez, A.E., Ondov, J.M., 2002. Ambient aerosol concentrations of elements resolved by size and by source: Contributions of some cytokine–active metals from coal– and oil–fired power plants. *Energy & Fuels* 16, 562–568.